

RADIATION DAMAGE IN TRIPALMITIN LAYERS STUDIED BY MEANS OF INFRARED SPECTROSCOPY AND ELECTRON MICROSCOPY

W. BAUMEISTER, U. P. FRINGELI, M. HAHN,
F. KOPP, and J. SEREDYNSKI

From the Institut für Biophysik und Elektronenmikroskopie der Universität Düsseldorf, West Germany; Laboratorium für Physikalische Chemie der Eidgenössischen Technische Hochschule, and Institut für Zellbiologie der Eidgenössischen Technische Hochschule, Zürich, Switzerland

ABSTRACT Structural deteriorations in biomembranes, as inevitably induced while structural information is gathered by electron optical methods, were evaluated by infrared spectroscopy. Tripalmitin model membranes were irradiated with 100 keV-electrons in an electron microscope. The intensity decay of group vibrations over the dose reveals the sequence of damage in the polar and nonpolar part of the molecule. The C—C backbone, being the most important structural feature, shows a significant latency effect up to $0.6 \text{ e}^-/\text{\AA}^2$ and is completely disordered by $3 \text{ e}^-/\text{\AA}^2$, corresponding to about three inelastic processes per molecule.

INTRODUCTION

Progress in molecular microscopy is, most fundamentally, limited by radiation damage. To evaluate realistic perspectives for determination of biomolecular structures at high resolution it is necessary to measure the kind and degree of inevitable structural alterations during exposure to the imaging electron beam. Very little is at present known about the degradation of biomembrane constituents by ionizing radiation and the resulting perturbations of the supramolecular organization of membranes. Experiments with simple well-ordered model membranes have shown that the radiation doses necessary for obtaining high resolution micrographs and for detection of single heavy atoms completely randomize molecular order and that the labeling heavy atoms—liberated by bond scissions—freely migrate and rearrange without resemblance to their initial pattern (Baumeister and Hahn, 1972, 1973). Thus all relevant information on the original molecular arrangement is destroyed before the micrograph is taken. Even electron diffraction studies of lipid layer systems require delicate techniques to avoid fading of the diffraction spots prior to recording (Glaeser and Deamer, 1969) though the doses needed for diffractograms are several orders of magnitude lower than those needed for high resolution imaging.

Molecular degradation of organic materials in the electron microscope has been investigated by numerous assays, particularly by measuring the total loss of mass, loss of

specific elements, loss of crystallinity, changes in optical and energy loss spectra, and changes in the images. The latter method to assess radiation damage by correlation between successive images (Frank et al., 1974), i.e. images obtained with increasing total specimen doses provides at least in principle the most relevant information in our context indicating those structural alterations which are within the resolution limits of imaging. It is however a principal drawback that no picture can be taken at zero total dose and that already the first picture (control) may suffer from manifest deteriorations. To trace back the original undisturbed structure would require a sound knowledge of the deterioration processes involved, which at present does not exist. Monitoring radiation damage by measuring fading of distinct spots in the diffraction pattern is restricted to periodic specimens, and moreover the situation of a molecule in a crystal must not necessarily reflect its reaction to ionizing radiation in a noncrystalline modification of the same material. Due to cage and surface effects different secondary decay processes may occur in the crystalline as compared with the amorphous state. Furthermore it is extremely difficult to assign the intensity loss of electron diffraction spots to distinct structural changes on a molecular level. Energy loss spectra provide valuable informations about different aspects of radiation damage: damage corresponding to defined electron excitations (0–10 eV range), mass loss, and changes in the relative elementary composition (Isaacson, 1975).

Infrared absorption spectra provide quantitative data on the destruction or formation of particular types of bonds during irradiation and moreover are a sensitive probe for changes of the molecular conformation. Conformational changes may be neglected at moderate resolution levels but become increasingly important at higher resolutions where most of them must be expected to be well within the limits of detectability. It is a certain drawback that the IR measurements are performed outside the electron microscope's vacuum which may lead to oxidative changes of the irradiated specimens. In most cases, however, these changes are discernible from the *in vacuo* radiation effects and can be related back to changes that have occurred inside the electron microscope. It should also be mentioned that using tunneling spectroscopy infrared as well as Raman spectra can also be obtained quasi on-line inside the microscope (Parikh, 1974). Infrared spectroscopy which has already earlier been used to study the degradation of synthetic and biogenic polymeres (Brookes, 1957; Reimer, 1965; Bahr et al., 1965) works for aperiodic as well as for periodic specimens and thus allows one to study possible differences in the behavior of the different phases (crystalline and noncrystalline) on the degradation process. Very small quantities of material are needed (less than 10 μg) and using the internal reflection (attenuated total reflection, ATR) technique, extremely thin (less than 100 Å) layers can be investigated. This has the advantage of similarity (*a*) of the test specimen to real electron microscopic preparations, especially membraneous layer systems, and (*b*) of the radiation energy transfer processes to the conditions of real electron microscopy and diffraction.

Preliminary experiments with Langmuir-Blodgett type tripalmitin layer systems had indicated that it may well be possible by means of this technique to study the sequence of the destructive process (Hahn et al., 1974). Sequence here is not to be understood as

the complex sequence of events following a given elastic and—more frequently and seriously—inelastic scattering process which finally leads to manifest chemical alterations but as the sequence of the destruction of distinct molecular groups reflecting their different radiation sensitivity, the sequence of recombination, and the sequence of conformational changes induced and propagated by local structural alterations of individual molecules.

MATERIALS AND METHODS

Deposition of Monolayers on Germanium Plates

Monomolecular layers were formed at the water-air interface of a Langmuir-type film balance by spreading arachidic acid (Fluka AG, Buchs, Switzerland) on a subphase containing 2×10^{-6} mol/liter CdCl_2 , 4×10^{-4} mol/liter KHCO_3 , and tripalmitin (Fluka) on quartz-distilled water. The temperature of the subphase as well as of the surrounding atmosphere was kept at $20 \pm 0.5^\circ\text{C}$. The transfer of the monolayers from the water-air interface to the germanium plates was performed according to the Langmuir-Blodgett technique (Blodgett, 1935; Blodgett and Langmuir, 1937) using a motor-driven dipping mechanism (transfer speed: 2.5 mm/min). The film balance was equipped with a servo-mechanism with integral-controller properties allowing any preset film pressure to be kept constant within $\pm 0.02 \text{ dyn} \cdot \text{cm}^{-1}$ during transfer to a solid support. Both Cd-arachidate and tripalmitin monolayers were transferred onto the germanium plates at film pressures of $20 \text{ dyn} \cdot \text{cm}^{-1}$. During the deposition the transfer ratio p (difference of film covered aqueous surface before and after deposition/geometrical surface of the solid support) was continuously monitored. The transfer ratios observed were always quite close to unity, thus assuring homogeneity of the layers as well as the deposition of equal amounts of sample material on the germanium plates.

The germanium plates exhibited a hydrophilic surface when thoroughly cleaned by ultrasonic treatment with methanol and water followed by plasma cleaning. Plates on which samples had been irradiated were in addition mechanically polished prior to this cleaning procedure in order to completely remove polymerized material.

First, one hydrophobizing Cd-arachidate layer was deposited on the germanium plates by withdrawing the plate from the subphase through the compressed film in order to obtain better transfer ratios p for the tripalmitin layers. Following this, eight layers of tripalmitin were deposited on top of the hydrophobizing interlayer by subsequent up and down cycles (y -type deposition according to Bikermann, 1940).

Because it was shown earlier (Kopp et al., 1975) that tripalmitin layers of the Langmuir-Blodgett type undergo a time-dependent spontaneous rearrangement from more or less homogeneous layers to randomly distributed microcrystals, the samples were stored for at least 48 h (in which time the mentioned rearrangement is nearly completed) at room temperature before irradiation. This avoided the possibility that changes of the spectra due to this rearrangement could interfere with changes of the spectra due to irradiation effects. Only a few samples were irradiated immediately after deposition to study the effects of irradiation on the rearrangement process and to reveal whether or not the radiation sensitivity depends on different molecular arrangements.

Irradiation

The tripalmitin-coated germanium plates were inserted into a device, which allowed to shift them under a stationary metal frame in the image plane of an electron microscope (Siemens Elmiskop Ia). Successively the plates were moved under the window of the frame allowing the electron beam to irradiate the samples with increasing doses. The incident current density was

obtained by measuring the total current I_m spread over a homogeneously illuminated circular area of diameter b . Regarding the efficiency $\gamma < 1$ (Grubb, 1971) of the built-in image current meter, which uses the insulated final screen as electron collector, the incident current density was $j = 4I_m/\pi b^2\gamma$. By keeping current densities j below $5 \times 10^{-8} \text{A}\cdot\text{cm}^{-2}$, any risk of a temperature rise above room temperature was avoided. Before irradiation the gun was allowed to reach a steady state, i.e. to deliver a constant current I_m . The vacuum was always better than 2×10^{-5} torr. Since there were no detectable differences between (non-irradiated) control samples kept in close vicinity of irradiated samples and those which had not been exposed to the electron microscope's vacuum it could be excluded that hydrocarbon deposits contributed to the characteristics of the spectra. 100 kV accelerating voltage was chosen to minimize multiple scattering in the sample and to study radiation damage under conditions comparable to today's high resolution electron microscopic work.

Dosimetry on Solid Supports

ATR-IR spectroscopy demands depositing of the specimen on the surface of a Ge-plate by far too thick to be penetrated by 100 keV electrons. To compare the effective doses acting on the thin ($\leq 10^{-5} \text{g}\cdot\text{cm}^{-2}$) specimen resting on the impenetrable solid with the doses collected by the same specimen in transmission electron microscopy on supports of approximately $10^{-6} \text{g}\cdot\text{cm}^{-2}$, the dose due to backscattered electrons (b.e.) has to be accounted for.

If $\sigma_k(E)$ is the cross-section for an interaction of kind k , dependent on the electron kinetic energy E , and for every incident primary electron (p.e.) we count η b.e. (η = backscattering yield factor) with normalized probability distributions $P_\vartheta(\vartheta) \sin \vartheta d\vartheta d\varphi$ over the angle ϑ relative to the normally incident p.e. with $P_{\vartheta \text{ p.e.}} = \delta(\vartheta = 0)$ and $P_E(E/E_b; \vartheta) d(E/E_b)$ relative to the monoenergetic p.e. with $P_{E \text{ p.e.}} = \delta(E = E_b)$ we can define a factor $f_k = D_{k\text{eff}}/D_n$ converting the nominal doses D_n applied to the Ge-plates into effective doses $D_{k\text{eff}}$ yielding

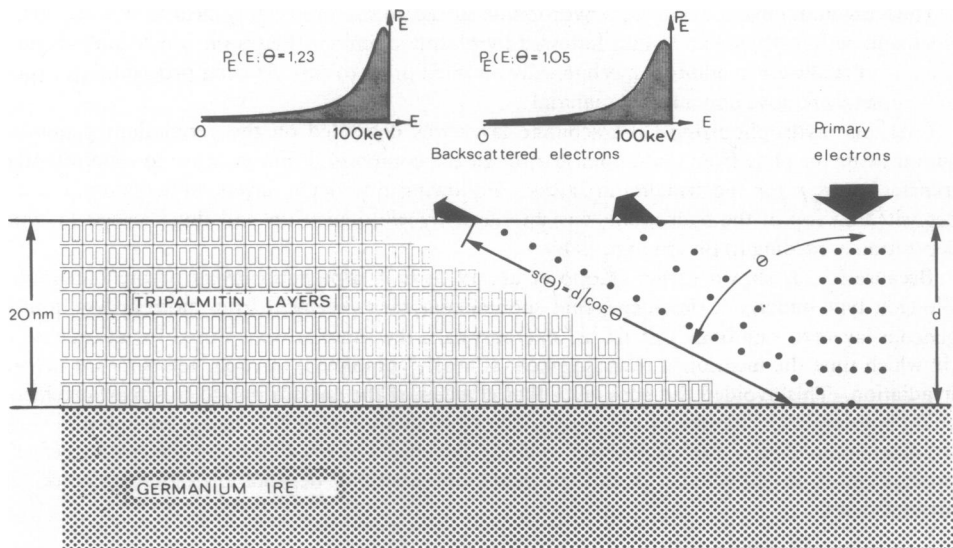


FIGURE 1 Geometry of irradiation of tripalmitin layers on a germanium internal reflection element (IRE). The number of dotted lines symbolizes the relative number of backscattered electrons to primary electrons, the distance between dots symbolizes the relative mean free paths between damaging events.

the same effects in case of one-way transmission of p.e. For normally incident p.e., P_ϑ is independent on azimuth; moreover we set $d\Omega = \sin \vartheta d\vartheta d\varphi$ and obtain

$$f_k = 1 + \eta[\sigma_k(E_b)]^{-1} \int_0^{2\pi} \int_0^{E_0} \sigma_k(E) P_E(E/E_b; \vartheta) P_\vartheta(\vartheta) (\cos \vartheta)^{-1} dE d\Omega. \quad (1)$$

For numerical evaluation, P_E and P_ϑ were fitted to experimental data (Kanter, 1957; Kulenkampff and Spyra, 1954) by generalized Lorentzian and Lambert distributions. $\eta(\text{Ge}; 100 \text{ keV}) = 0.313$ is also known from measurements (Drescher et al., 1974) (Fig. 1).

ATR-IR Spectroscopy

For a detailed discussion of ATR-IR spectroscopy the reader is referred to Harrick (1967).

The spectra were scanned with polarized light from $4,000 \text{ cm}^{-1}$ to $1,000 \text{ cm}^{-1}$ with a Perkin-Elmer infrared spectrometer (model 225, Perkin-Elmer Corp., Norwalk, Conn.), equipped with a KBr-grid polarizer. Two Ge-internal reflection plates ($50 \times 20 \times 1 \text{ mm}$) were used, with an angle of incidence of 30° . By this means one obtains about 85 internal reflections. The temperature of the plates was kept at $18 \pm 0.5^\circ\text{C}$ during the scans (Fig. 2).

Electron Microscopy

Some of the lipid-covered germanium ATR reflection plates were prepared for electron microscopic investigation after the infrared scans of them had been taken. For this purpose the samples were replicated in a Balzers freeze-etch device BA 500 M (Balzers AG, Liechtenstein), as described previously (Kopp et al., 1975). To avoid condensation, the vacuum was broken only when the samples were again at ambient temperature. Squares of about 1 mm^2 were scratched into the replica with a fine needle and the replicas were then floated onto a clean water surface. This last step was sometimes not very easy to achieve since the replicas, particularly those of samples that had been irradiated, showed a strong tendency to stick to the lipid-covered germanium plate. It was found that soaking the plates in a detergent solution at 40°C for several hours helped in the most resistant cases. The lipid remnants adhering to the replicas did not contribute significantly to the contrast in the electron microscope so that we could avoid any further cleaning. The replicas were picked up with Formvar-coated EM grids, reinforced with about 10 nm of carbon. The micrographs shown in this paper have been photographically reversed so that the evaporated platinum appears white, whereas the shadows are black. The micrographs are arranged in such a way that the shadowcasting direction is approximately from top left to bottom right.

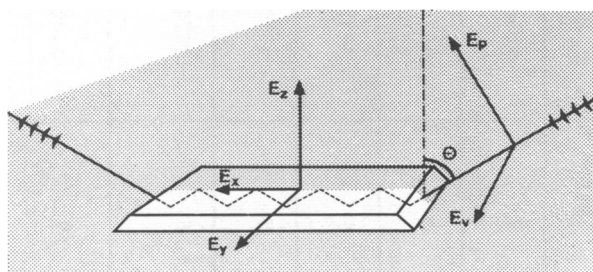
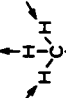
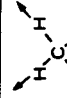
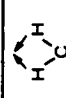
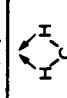
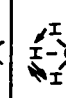
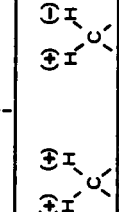

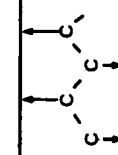


FIGURE 2 ATR set up. θ , angle of incidence. E_p , E_v , parallel and perpendicular polarized components of the electric field of incident light. E_x , E_y , E_z , electric field components with respect to the coordinate system corresponding to the internal reflection plate ($E_p \rightarrow E_x$, E_z , $E_v \rightarrow E_y$).

TABLE I
SYNOPSIS OF VIBRATION MODES SELECTED FOR QUANTITATIVE COMPARISON OF DECAY RATES

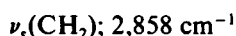
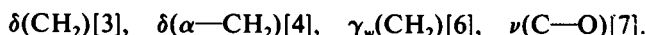
Vibration mode no.	Wavenumber [cm ⁻¹]	Assignment	Stylized vibration mode	Remarks
1	2960	ν_a (CH ₃)		antisymm. CH-stretching of CH ₃ groups
2	2858	ν_s (CH ₂)		symm. CH-stretching of CH ₂ groups
3	1472	δ (CH ₂)		methylene bending of hydrocarbon chain
4	1419	δ (α -CH ₂)		bending of α -methylene groups
5	1370	δ_s (CH ₃)		symm. bending of methyl groups
6	1220	γ_w (CH ₂) and γ_t (CH ₂)		typical band from the wagging and twisting sequence of methylene groups in all-trans-configuration
7	1180	ν (C-O)		group vibration of R - C(=O) - R with CO-single bond stretching involved typical for crystalline configuration
8	1112	ν (C-C)		stretching of C-C frame of hydrocarbon chains

RESULTS AND DISCUSSION

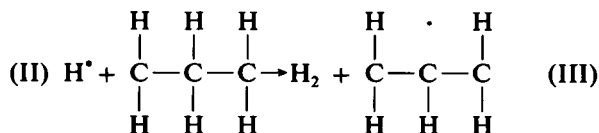
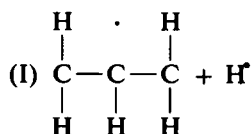
Table I summarizes the group vibrations which have been selected to monitor the degradation of tripalmitin in the polar as well as in the nonpolar part of the molecule during irradiation. It should be mentioned, however, that the term "group vibration" is only an approximation to the real behavior because generally all atoms are involved in a vibrational mode. For the selected group vibrations, however, it has previously been shown (Bellamy, 1968; Zbinden, 1964; Fringeli et al., 1972) that they are only weakly influenced by the rest of the molecule. The group vibrations listed in Table I can roughly be divided into relatively (I) conformation independent:



and (II) typical conformation-dependent group vibrations:



The decrease in the intensity of the C—H stretching modes of the methylene groups might be either due to elimination of hydrogen by C—H bond scission or to fragmentation of the main chains (C—C bond scissions) followed by evaporation of fragments. If the latter mechanism prevails this would imply that the decay of $\nu_s(\text{CH}_2)$ is accompanied by a loss of total mass. This can however be excluded, at least up to doses of $0.6 \text{ e}^-/\text{\AA}^2$, since there is no decrease in the intensity of the C—C frame stretching. Also electron microscopy (see Fig. 7) ascertains that no considerable mass loss takes place up to these doses. The micrographs, however, clearly show that the contours of the tripalmitin microcrystals are smooth which could tentatively be interpreted as caused by some mass loss at the crystal edges, probably energetically favored. Thus we conclude that the decrease in $\nu_s(\text{CH}_2)$ intensity is mainly due to hydrogen elimination. If C—H bond scission is the predominant effect of irradiation the liberated hydrogen atom may subsequently undergo H-abstraction from another main chain to form another radical and H_2 . Reactions between main chains may give cross-links:



I + II cross-link

TABLE II
REGRESSION OF VIBRATION MODES

Vibration mode no.	Assignment	$a(D)=a_0-a_1D$ regression* $n = \frac{a_1}{a_0} \left[\frac{D^2}{e^{-D}} \right]$
1	$\nu_a(\text{CH}_3)$	$- 0.355 \pm 0.200$
2	$\nu_g(\text{CH}_2)$	$- 0.353 \pm 0.068$
3	$\delta(\text{CH}_2)$	$- 0.516 \pm 0.092$
4	$\delta(\alpha\text{-CH}_2)$	$- 0.503 \pm 0.080$
5	$\delta_g(\text{CH}_3)$	$- 0.269 \pm 0.158$
6	$\nu_w(\text{CH}_2)$ $\nu_t(\text{CH}_2) \ 0 - 2.0 \ e^{-D}/D^2$	$- 0.511 \pm 0.096$
	$\nu_w(\text{CH}_2)$ $\nu_t(\text{CH}_2) \ 0 - 0.5 \ e^{-D}/D^2$	$- 0.176 \pm 0.487$
	$\nu_w(\text{CH}_2)$ $\nu_t(\text{CH}_2) \ 0.5-2.0 \ e^{-D}/D^2$	$- 0.518 \pm 0.186$
7	$\nu(\text{C-O})$	$- 0.456 \pm 0.122$
8	$\nu(\text{C-C})$	$- 0.450 \pm 0.120$
	$\nu(\text{C-C}) \ 0 - 0.6 \ e^{-D}/D^2$	$- 0.024 \pm 0.237$
	$\nu(\text{C-C}) \ 0.5-2.0 \ e^{-D}/D^2$	$- 0.504 \pm 0.081$

* The errors indicated are related to 99 % fiducial limit.

$\nu_a \text{CH}_3$ and $\delta_s(\text{CH}_3)$; 2,960 cm^{-1} , 1,370 cm^{-1}

Both vibrations are known to be isolated motions of the methyl groups. Nevertheless their sensitivity to ionizing radiation differs significantly (see Table II). Two explanations can be given at present:

(A) It is known (Fringeli et al., 1972; Münch et al., 1976) that $\nu_a(\text{CH}_3)$ is still to some degree dependent on intermolecular interactions. In crystalline stearic acid $\nu_a(\text{CH}_3)$ is split in two due to this interaction. With $\delta_s(\text{CH}_3)$ no splitting is observed. This means that the latter group vibration gives the more relevant information on the destruction of methyl groups. This finding is supported by infrared spectroscopic investigations of polymers, where $\delta_s(\text{CH}_3)$ was used to determine the degree of chain branching (Cross et al., 1950). Since conformation-dependent group vibrations should generally show a higher radiation sensitivity due to propagation of conformational changes by local chemical alterations this could explain the observed discrepancy in the

radiation sensitivity. If this holds true, i.e., if $\delta_s(\text{CH}_3)$ gives the more relevant information on the methyl-group destruction, then the methyl group must obviously be considered as being the most resistant group within the whole tripalmitin molecule. This might in turn be interpreted as: (1) Relatively efficient restoration at the endpoints of broken and branched main chains. It should however be mentioned that if this mechanism works an increase of CH_3 -group vibrations should be expected for polymers—where most of the fragments are nonvolatile. This has hitherto not yet been observed. It might, however, be possible that in tripalmitin layers H^\bullet radicals preferentially diffuse laterally in the plane between neighboring hydrophobic planes, i.e. in the

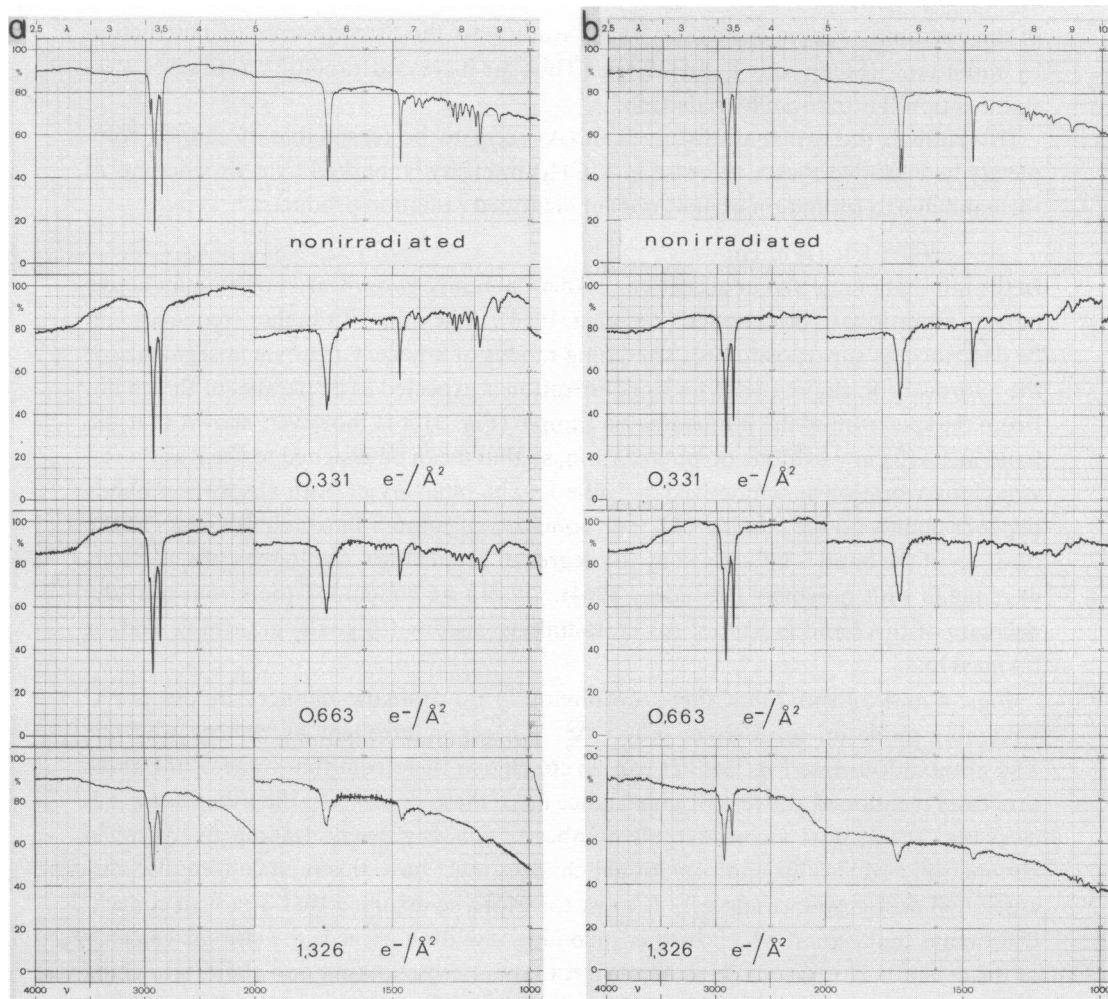
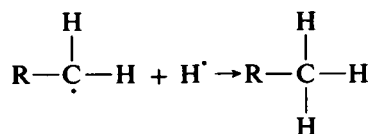


FIGURE 3 ATR-IR spectra of eight tripalmitin layers deposited on a germanium IRE and irradiated with increasing 100 keV-electron doses. (a) Parallel polarization; (b) perpendicular polarization.

center of a "bilayer." This would for our special molecular arrangement increase the probability for methyl-group restoration



(2) Alternatively the relative resistance of the methyl group could be explained by hyperconjugation of the methyl group with free radicals generated in the aliphatic chain which induces π -type bonds in the methyl group (Hedvig, 1972). Because π -bonds more easily dissipate excess energy (Spehr and Schnabl, 1973), the radiation sensitivity of the remaining system is smaller, finally leading to the "steady-state of destruction by radiation" (Stenn and Bahr, 1970). Thus an increased radiation resistance (" π -stabilization") is induced by radiation.

(B) Though the explanations given in (A) seem to be reasonable, it cannot completely be excluded that a decrease in $\delta_s(\text{CH}_3)$ intensity is masked by a broadening of the band due to formation of new, not yet identified radiation products.

$$\nu(\text{C}-\text{C}): 1,112 \text{ cm}^{-1}$$

In the infinitely long planar zigzag chain there are only two infrared or Raman active normal vibrations to be expected (Zbinden, 1964). The one with higher frequency can be described as superposition of stretching modes of adjacent methylene segments of the hydrocarbon chain, therefore its polarization is expected to be parallel to the chain. From the spectrum of the nonirradiated sample (Fig. 3) it is, however, shown that the band at $1,112 \text{ cm}^{-1}$ exhibits no polarization, so that it can be assigned to the transversal stretching vibration as symbolized in Table I. The intensity of both absorption bands depends mainly on the number of C—C bonds arranged in a linear chain, whereas the position of the band is influenced by the degree of branching. Analogous observations were made with polymers (Zbinden, 1964). It can be concluded therefrom that the decrease of this band indicates: (a) cross-linking and/or (b) chain branching and/or (c) mass loss.

Figs. 4 and 5c show that there are obviously no dramatic changes in the C—C stretching mode up to doses of $0.6 e^- / \text{\AA}^2$. This is in excellent agreement with the EM observations (see Fig. 7a). It can be concluded therefrom that none of the three processes mentioned above is of importance up to these doses. On the other hand it is clear that at this dose a considerable number of ionizing events leading to hydrogen elimination and various conformational changes must have taken place (see also discussion of dose-response curves). It must therefore be assumed that a radical concentration has built up, at which further incoming radiation exceeds the storage capacity of the crystal. This gives rise to an abrupt massive cross-linking and chain branching in the inner part of the crystal where the probability for various types of recombination is increased as compared to the surface. This hypothesis would be consistent with the latent-dose concept suggested by Siegel (1972). Electron microscopy reveals a smoothing of the crystal edges from which it can be concluded that chain-fragments

produced near to the surface evaporate. Cage effects within the crystal favor recombination (up to moderate dose obviously predominantly quasi-isomorphous recombinations) and at higher doses random cross-linking.

$$\delta(\text{CH}_2), \delta(\alpha\text{-CH}_2), \gamma_w(\text{CH}_2); 1,472 \text{ cm}^{-1}, 1,419 \text{ cm}^{-1}, 1,220 \text{ cm}^{-1}$$

Generally it can be seen from Table II that the molecular conformation is considerably more sensitive to irradiation than other structural features. As conformational changes must be regarded to be indirect radiation effects this clearly indicates that ionizing events at a given point of a tripalmitin molecule might cooperatively disturb

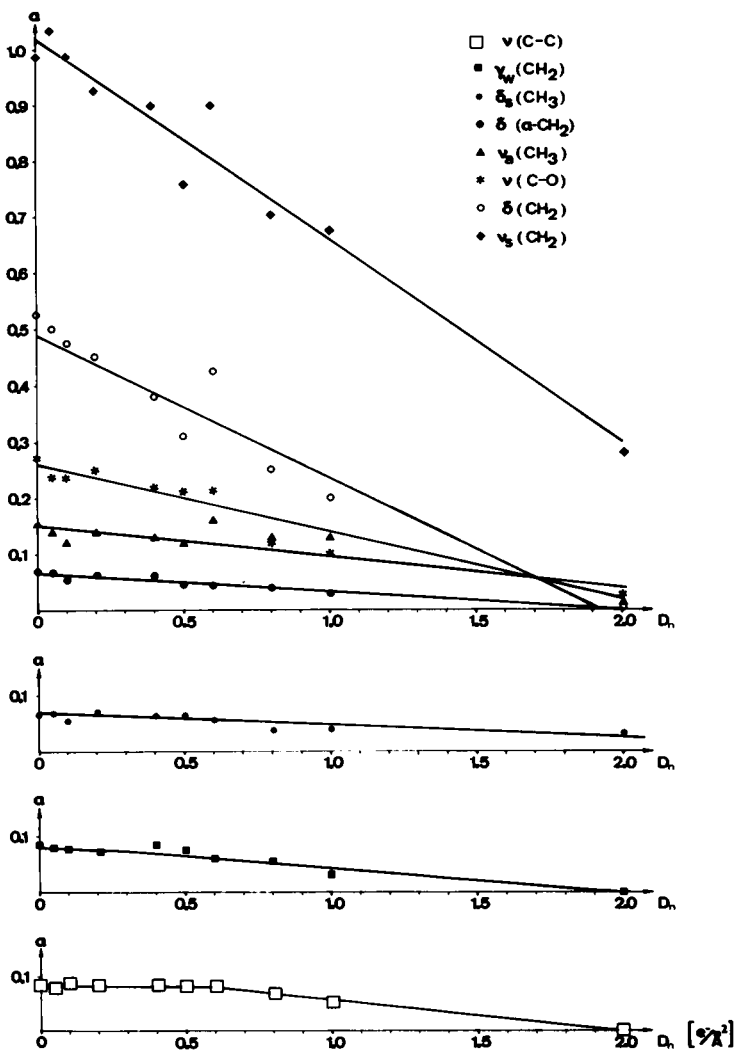


FIGURE 4 Absorption coefficients α for various characteristic vibration modes as a function of the primary electron dose D_n as experimentally applied to the preparations.

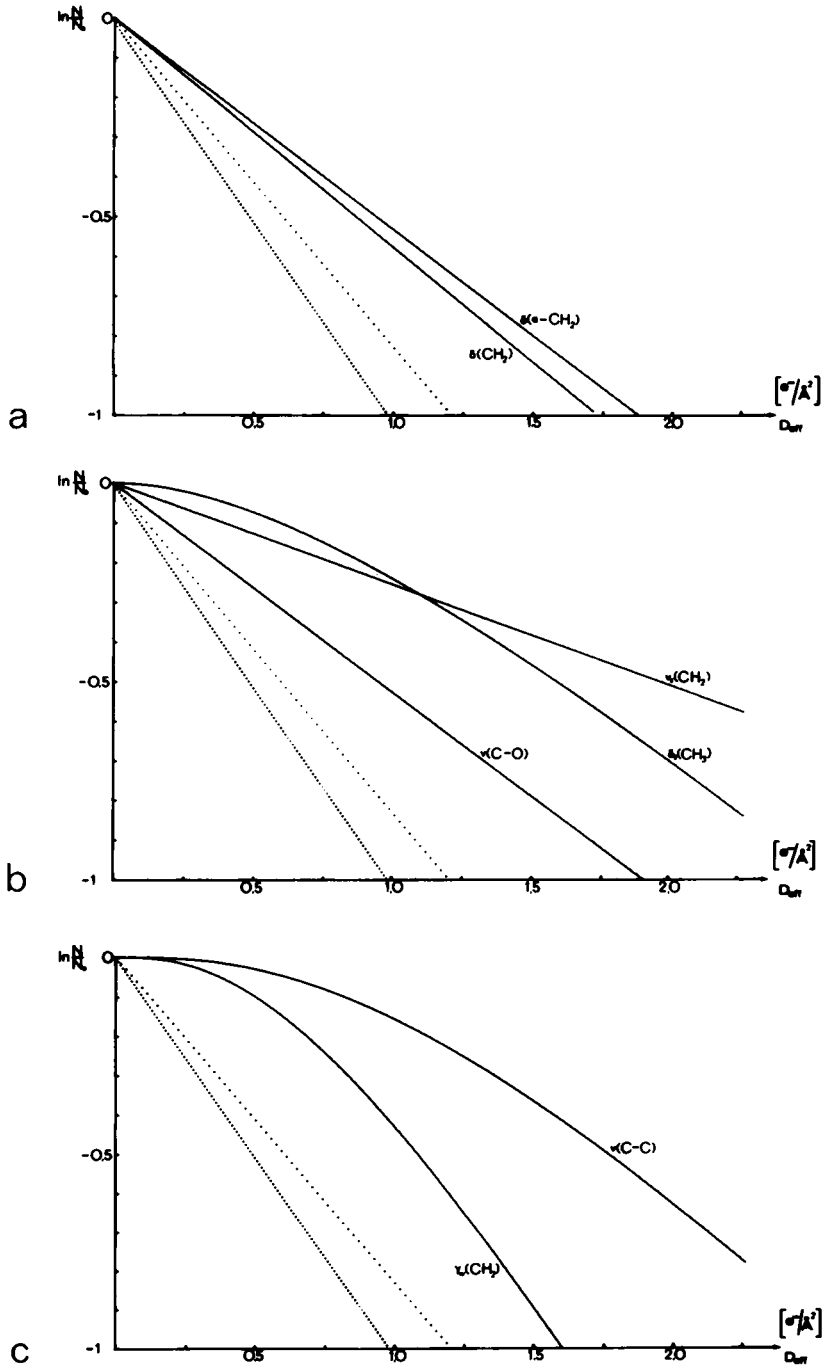


FIGURE 5 *a-c* Semilog plots of normalized absorption coefficients N/N_0 over the doses converted for single transmission of 100 keV-electrons. (See Eq. 1) fraction of molecules without inelastic event; ... fraction of molecules without ion cluster.

the conformation within extended volumes of the crystal. All three group-vibrations are sensitive probes indicating deviations in the hydrocarbon chain from the all-*trans*-configuration. While the $\delta(\text{CH}_2)$ and the $\gamma_w(\text{CH}_2)$ group vibrations are of equal sensitivity the $\delta(\alpha\text{—CH}_2)$ group exhibits a slightly lower sensitivity. However no proof can yet be given that the conformation dependence of $\delta(\text{CH}_2)$ and $\delta(\alpha\text{—CH}_2)$ are identical. If $\delta(\alpha\text{—CH}_2)$ is really more resistant this might be ascribed to π -character of the neighboring carbonyl group (see also $\nu(\text{C—O})$). The rate of decay of $\gamma_w(\text{CH}_2)$ seems to be accelerated by the abrupt breakdown of the C—C backbone upon reaching the critical radical storage capacity.

$$\nu(\text{C—O}); 1,180 \text{ cm}^{-1}$$

Also this vibration is strongly conformation dependent and reflects the order-disorder in the polar part of the molecule. It is observed at $1,180 \text{ cm}^{-1}$ if the atoms of the COO group and the C atoms of the adjacent CH_2 groups are in plane. Deviations from this conformation will shift the bands to lower wavenumbers, followed by a change in the polarization (Fringeli et al., 1972). The sensitivity to radiation damage seems to be significantly lower in the polar part of tripalmitin as compared to the hydrocarbon chains, which, considering the above stated facts, might be ascribed to the π -character of the carbonyl group.

$$\nu(\text{C=O}); 1,738 \text{ cm}^{-1}, 1,730 \text{ cm}^{-1}$$

This prominent absorption band can be assigned to the carbonyl-stretching mode. The splitting observed in the spectrum of the nonirradiated sample reflects the C_s symmetry in the polar part. Though broadening of the band due to loss of C_s -symmetry is clearly recognizable in the spectra (see Fig. 3) a quantitative analysis of the band was not performed, because of overlapping of the absorption bands of tripalmitin in crystalline and in deteriorated conformations.

$$\nu(\text{C=C}); 1,620\text{--}1,680 \text{ cm}^{-1}$$

We have not been able to detect the formation of absorption bands which could be assigned to C=C stretching vibrations. Nevertheless we can not exclude the formation of double bonds because it is known that the corresponding absorption bands may be very weak (Bellamy, 1968). Moreover it is to be expected that due to the stochastic distribution of C=C bond positions determining the frequency, the bands are smeared. On the other hand the absence of C=C bonds could also be due to the fact that C=C bonds are active sites for the trapping of radicals. They therefore can be expected to exist mainly as transients. Furthermore remaining C=C bonds could be eliminated by oxidation between irradiation and the measurement of the infrared spectrum. Here again it cannot be excluded that the absorption bands to be expected for the corresponding oxidative products are obscured by interfering with stronger absorption bands from the ester part of the molecule.

Discussion of Dose-Response Curves

In radiation biology, a sigmoid appearance of semilog dose-response curves is considered as proof for multistep damaging processes. Already from the linear regres-

TABLE III
WEIGHTED APPROXIMATION OF DECAY CURVES
ACCORDING TO EQS. 2 AND 3

No.	Vibration mode assignment	Formal 'cross-section' b [g^2]	Formal 'number of targets' m	Quality of approximation Δ^2
1	$\nu_a(\text{CH}_3)$	0.117	1	0.069
2	$\nu_b(\text{CH}_2)$	0.256	1	0.022
3	$\delta(\text{CH}_2)$	0.579	1	0.029
4	$\delta(\alpha\text{-CH}_2)$	0.534	1	0.025
5	$\delta_b(\text{CH}_3)$	0.623	2	0.047
6	$\gamma_w(\text{CH}_2)$	1.22	3	0.016
7	$\nu(\text{C-O})$	0.529	1	0.023
8	$\nu(\text{C-C})$	0.751	3	0.010

sions (see Table II) it is apparent that for some vibration modes a latency dose must be exceeded until decay starts. To show these effects more quantitatively, we approximated their normalized absorption coefficients $N/N_o(D_{\text{eff}})$ by

$$F(b; m) = 1 - [1 - \exp(-b D_{\text{eff}})]^m, \quad (2)$$

with integer $m > 0$ (Dertinger and Jung, 1970). F is known from stochastics of radiation effects to describe dose-responses for one-hit in m targets. Although the interpretation of vibration decay is obviously not possible in elementary terms of target theory, F was used because it allowed a better approximation as a (more complicated) expression for multi-hit, one-target responses. Because the accuracy of measurements decreased with the absorption values at higher doses, N/N_o was taken as weight factor for the minimization of the square error sum.

$$\Delta^2 = \sum_i \{[N/N_{o_i}(D_{\text{eff}_i}) - F_i(b; m)]N/N_{o_i}\}^2. \quad (3)$$

For five of eight vibration modes $\Delta^2 \rightarrow \min$ led to simple exponential decay functions, i.e. $m = 1$; the sigmoid appearance of the remaining dose-responses demanded $m > 1$ (see Table III).

At least the $\nu(\text{C-C})$ and $\gamma_w(\text{CH}_2)$ vibrations show a distinct sigmoidicity, which tentatively can be interpreted as due to multistep damaging processes in which cooperative interactions between single molecules might be involved. The slightly sigmoid

appearance of $\delta_1(\text{CH}_3)$ confirms the above stated hypothesis that the relative resistivity of this group is due to a repair mechanism which seems to become less efficient as soon as the supramolecular organization breaks down. (H^+ -diffusion in the bilayer planes.)

To compare the measured decay of a given vibration mode with the number of inelastic scattering events to be expected per tripalmitin molecule, we calculated the cross section for inelastic scattering:

$$\sigma_{\text{in}}(E_b) = \frac{3}{4}(\lambda_c^2/\pi\beta^2) \sum_i (Z_i)^{1/2} (\ln B - \beta^2), \quad (4)$$

with λ_c = Compton-wavelength = $2.425 \times 10^{-2} \text{ \AA}$; β = electron velocity/velocity of light; $B = (2E_o\beta/E_1)[E_b(2 + E_b/E_o)E_o(1 - \beta^2)]^{1/2}$; and $E_1 = 37 \text{ eV}$ = mean inelastic energy loss, $E_o = 511.3 \text{ keV}$ = rest energy of the electron, and $E_b = 100 \text{ keV}$ = acceleration energy of the beam electrons. The numerical factor was fitted to measurements on thin biogenic solid specimen (Isaacson, 1972).

Computation of Eq. 1 with this $\sigma_{\text{in}}(E)$ yields $f_{\text{in}} = 1 + 1.09$ and a total cross section $\sigma_{\text{in}} = 1.02 \text{ \AA}^2$ for one tripalmitin molecule and $E_b = 100 \text{ keV}$.

As another approach we summed up the gross-ionization cross sections (Schram et al., 1965),

$$\sigma_{\text{ig}} = (\lambda_c^2 M_i^2/\pi\beta^2)[\ln(c_i E_o^2/2(1 - \beta^2)) - \beta^2], \quad (5)$$

with the coefficients for the listed bond types (Table IV), taken from measurements on gaseous hydrocarbons (Schram et al., 1966). Because the decay of the different vibrations cannot in a straightforward manner be ascribed to the scission of a single bond type, we computed the dose conversion factor $f_{\text{ig}} = 1 + 1.135$ as a weighted mean for the 98 C—H, the 56 (C—C and C—O), and the 3 π (C—O) bonds, although the different voltage coefficients yielded slightly different values for the three bond types. For the same reason one cannot expect similarity between σ_{ig} for different bonds and "cross sections" derived from semilog plots of single vibrations related to the bond type in question.

The gross-ionization cross section σ_{ig} (see Eq. 5) of a tripalmitin molecule was divided by the average number of 1.64 ion pairs generated per primary ionization ("cluster") (Ore and Larsen, 1964) yielding a cross section of $\sigma_{\text{cl}} = 0.832 \text{ \AA}^2$ for cluster generation by 100 keV-electrons. Both values (σ_{cl} and σ_{in}) coincide fairly well.

By chance ($\sigma_{\text{in}} \approx 1 \text{ \AA}^2$) the number of inelastic events per molecule is equal to

TABLE IV
GROSS-IONIZATION CROSS SECTIONS WITH
COEFFICIENTS FOR BOND TYPES

Bond	M_i^2	$c_i \cdot \text{eV}$
C—H	1.07	0.134
$\left. \begin{array}{l} \sigma(\text{C—C}) \\ \sigma(\text{C—O}) \end{array} \right\}$	2.5	0.0676
$\pi(\text{C—O})$	0.4	0.107

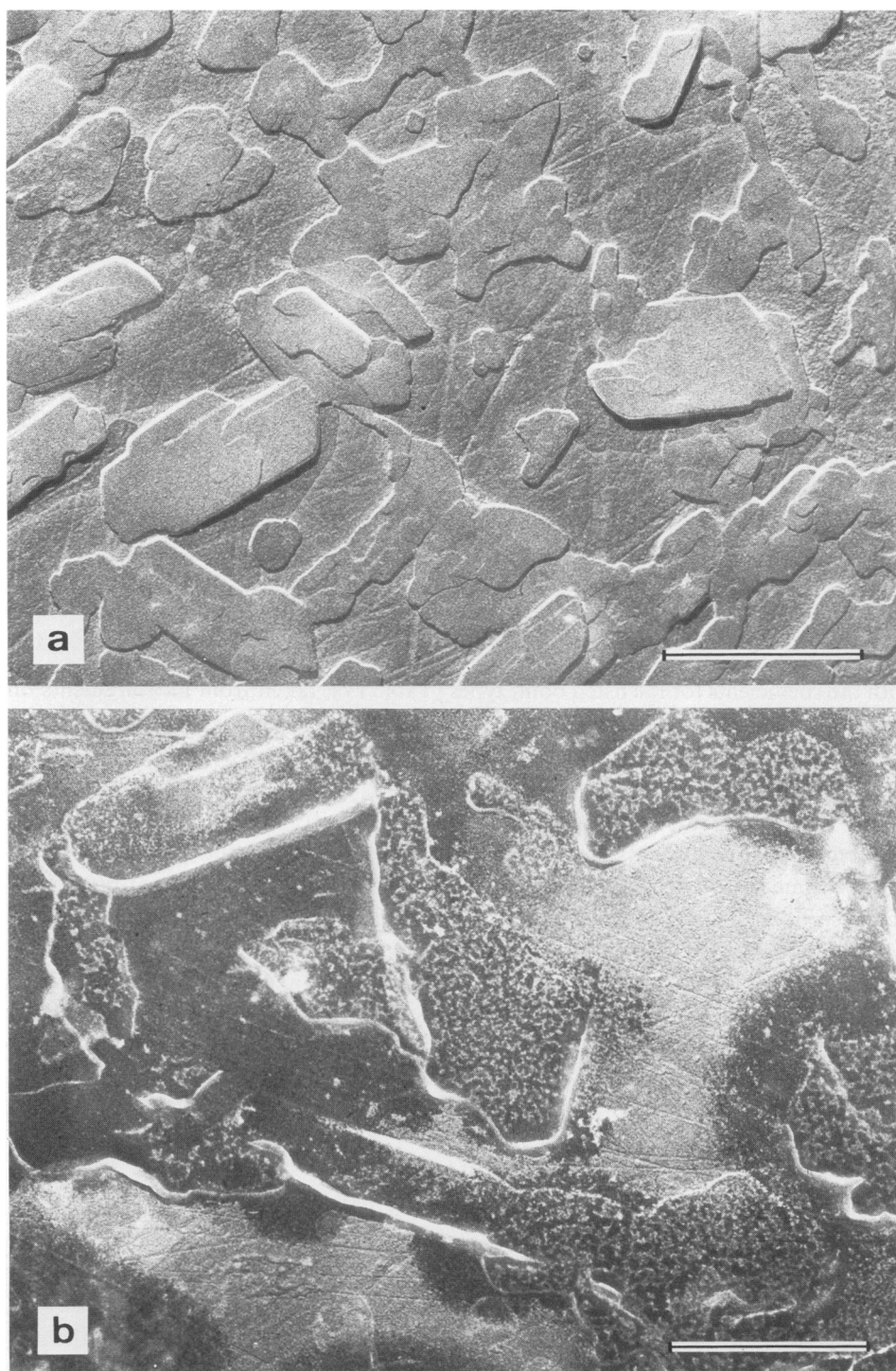


FIGURE 6 (a) Electron micrograph of a control specimen showing eight layers of tripalmitin after they had been aged for 48 h at 25°C. The original more or less homogeneous layers have rearranged into microcrystals. The germanium plates were polished optically plane. Scratches from the polishing can be seen on them. $\times 28,000$. (b) A similar specimen as in Fig. 6 a but after irradiation with $2.12 e^-/\text{\AA}^2$. Remnants of perforated crystals are recognizable. After this treatment the platinum no longer condenses homogeneously on the specimen. $\times 28,000$.

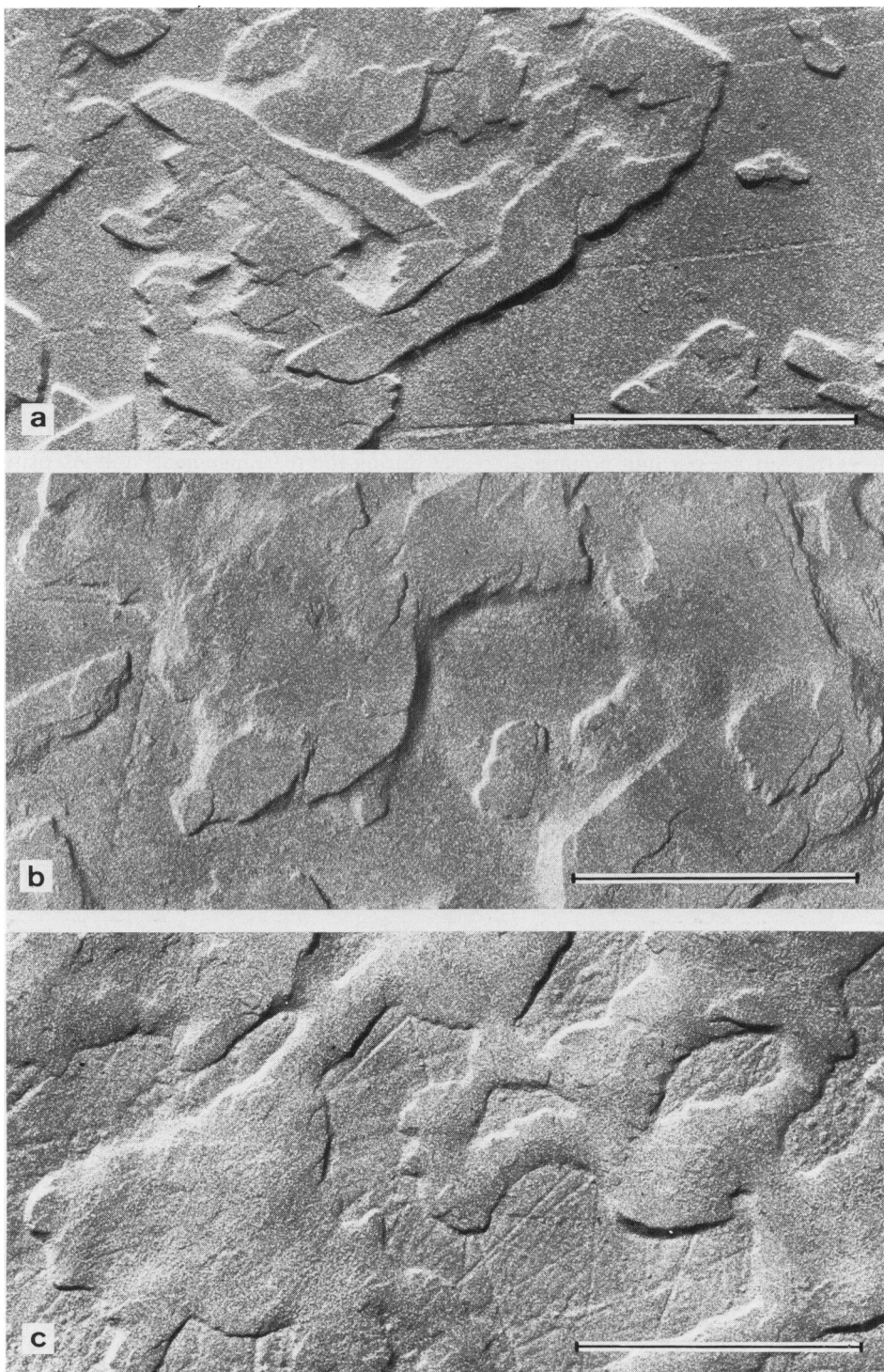


FIGURE 7 (a) At $0.6 e^-/\text{\AA}^2$ no significant differences are found when compared with the control (Fig. 6a). (b) Concomitant with the destruction of the C—C backbone (see Table II), ultrastructural changes are clearly seen at $0.8 e^-/\text{\AA}^2$. A smoothing of the crystal contours can be recognized which is even more pronounced in (c) where the dose was $1.07 e^-/\text{\AA}^2$. $\times 40,000$.

the effective dose in electrons/ \AA^2 in Fig. 5*a-c*, drawn according to a mean conversion factor $f_m = (f_{in} + f_{ig})/2 = 2.11$. Comparing the decay of the C—C backbone ($\nu(\text{C—C})$), which must be regarded as the most important structural feature in terms of electron microscopy, with the figures obtained for σ_{in} and σ_{ei} reveals that the radical storage capacity allows not more than about one primary event per molecule without noticeable structural disorder, while three events lead to nearly complete destruction of the original hydrocarbon chain.

Langmuir-Blodgett Layers vs. Microcrystals

From Langmuir-Blodgett layers irradiated immediately after deposition on the germanium plates, i.e. before they rearranged into microcrystals, some preliminary evidence was obtained that the liquid crystalline state is more radiation sensitive than the crystalline state. This may be attributed to the combined influence of surface effects (the surface per unit volume decreases during the rearrangement) and viscosity effects. The greater mobility of excited species in Langmuir-Blodgett layers increases the probability of random cross-linking and diminishes the probability of cage-recombination.

Electron Microscopic Observations

The electron micrograph in Fig. 6*a* shows a non-irradiated control specimen. Rearrangement of the originally Langmuir-Blodgett layers to a microcrystalline state has occurred. Fig. 6*b* shows a similar sample, but after it had been exposed to a dose of $2.12e^-/\text{\AA}^2$. The obvious destruction of the object shown by the replication technique is in good agreement with the results obtained by ATR-IR spectroscopy. The contours of the former tripalmitin crystals can still be recognized but they exhibit a foamlike perforated structure. In the samples that had been exposed to a dose of this amount we often found that the platinum did not condense homogeneously all over the sample, so that quite large areas of such samples appear black as shown in Fig. 6*b*. This observation seems interesting because it might be an example of "chemical decoration." Fig. 7 shows three samples of aged tripalmitin layers irradiated with intermediate doses. Ultrastructural changes could not be detected up to $0.6e^-/\text{\AA}^2$, although some hydrogen-elimination and drastic conformational changes had occurred as revealed by changes in the infrared spectrum. The abrupt breakdown of the C—C backbone, however, is accompanied by a concomitant breakdown of the ultrastructure (Fig. 7*b,c*) indicated by the flattening of the microcrystals and a smoothening of their contours.

The authors wish to thank Prof. Hs. H. Günthard, Prof. K. Mühlethaler, and Dr. R. E. Bühler for stimulating discussions, Mrs. M. Fringeli for performing spectroscopic measurements, Miss S. Wiedemann for statistical analysis, Miss M. Kikhoefer for monolayer preparations and Mrs. E. Ludolph for preparing the manuscript.

This work was supported by the Deutsche Forschungsgemeinschaft (project Ru 5/17), the Schweizerischer Nationalfonds (project no. 3.0570.73), and the Fritz Hoffman-La Roche Stiftung (project no. 127).

W. Baumeister also gratefully acknowledges the receipt of an EMBO short-term fellowship.

Received for publication 17 November 1975.

REFERENCES

- BAHR, G. F., F. B. JOHNSON, and E. ZEITLER. 1965. The elementary composition of organic objects after electron irradiation. *Lab. Invest.* 14:1115.
- BAUMEISTER, W., and M. HAHN. 1972. Imaging of heavy atom patterns in well defined monomolecular layers. Proceedings of the Fifth European Congress on Electron Microscopy, Manchester. Institute of Physics, London. 648.
- BAUMEISTER, W., and M. HAHN. 1973. Elektronenmikroskopische Untersuchungen bei atomarer Auflösung an Modellmembranen. *Cytobiologie.* 7:244.
- BELLAMY, L. J. 1968. Advances in Infrared Group Frequencies. Methuen, New York.
- BIKERMANN, J. J. 1940. Contact angles of built up multilayers. *Trans. Faraday Soc.* 36:412.
- BLODGETT, K. B. 1935. Films built by depositing successive monomolecular layers on a solid surface. *J. Am. Chem. Soc.* 57:1007.
- BLODGETT, K. B., and I. LANGMUIR. 1937. Built-up films of barium stearate and their optical properties. *Phys. Rev.* 51:964.
- BROCKES, A. 1957. Über Veränderungen des Aufbaus organischer Folien durch Elektronenbestrahlung. *Z. Phys.* 149:353.
- CROSS, L. H., R. B. RICHARDS, and H. A. WILLIS. 1950. Infrared spectrum of ethylen-polymers. *Disc. Faraday Soc.* 9:235.
- DERTINGER, H., and H. JUNG. 1970. Molecular Radiation Biology. Springer-Verlag, New York. Vol. 12.
- DRESCHER, H., E. R. KREFTING, L. REIMER, and H. SEIDEL. 1974. The orientation dependence of the electron backscattering coefficient of gold single crystal films. *Z. Naturforsch.* 29a:833.
- FRANK, J., S. M. SALIH, and V. E. COSSLETT. 1974. Radiation damage assessment by digital correlation of images. Proceedings of the Eighth International Congress on Electron Microscopy, Canberra. Australian Academy of Science. II:678.
- FRINGELI, U. P., H. G. MÜLDNER, H. H. GÜNTARD, W. GASCHÉ, and W. LEUZINGER. 1972. The structure of lipids and proteins studied by attenuated total reflection (ATR) infrared spectroscopy. I. Oriented layers of tripalmitin. *Z. Naturforsch.* 27b:780.
- GLAESER, R. M., and D. W. DEAMER. 1969. Biomolecular and monomolecular lipid films: selected area electron diffraction. Proceedings of the 27th Annual Meeting of the Electron Microscope Society of America. Clailor's Publishing Div. 338.
- GRUBB, D. T. 1971. The calibration of beam measurement devices in various electron microscopes, using an efficient Faraday cup. *J. Phys. E. Sci. Instrum.* 4:222.
- HAHN, M., U. P. FRINGELI, and W. BAUMEISTER. 1974. Radiation damage studies of membrane model systems by means of ATR-IR spectroscopy. Proceedings of the Eighth International Congress on Electron Microscopy, Canberra. Australian Academy of Science. II:672.
- HARRICK, N. J. 1967. Internal reflection spectroscopy. Wiley-Interscience Publishers, New York.
- HEDVIG, P. 1972. Theory of free radicals. In *The Radiation Chemistry of Macromolecules*. Malcolm Dole, editor. Academic Press, New York. 55.
- ISAACSON, M. 1972. The interaction of 25-keV electrons with guanine and cytosine. *Radiat. Res.* 49:63.
- ISAACSON, M. 1975. Specimen damage in the electron microscope. In *Principles and Techniques of Electron Microscopy*. Vol. 6. M. A. Hayat, editor. Van Nostrand Reinhold Company, New York. In press.
- KANTER, H. 1957. Zur Rückstreuung von Elektronen im Energiebereich von 10 bis 100 keV. *Ann. Phys.* 20:144.
- KOPP, F., U. P. FRINGELI, K. MÜHLETHALER, and H. H. GÜNTARD. 1975. Instability of Langmuir-Blodgett layers of barium stearate, cadmium arachidate and tripalmitin, studied by means of electron microscopy and infrared spectroscopy. *Biophys. Struct. Mech.* 1:75.
- KULENKAMPFF, H., and W. SPYRA. 1954. Energieverteilung rückdiffundierter Elektronen. *Z. Phys.* 137: 416.
- MÜNCH, W., U. FRINGELI, and H. H. GÜNTARD. 1976. Polarized IR-ATR-single crystal spectra of stearic acid d_0 and d_{35} . *Spectrochim. Acta*. In press.
- ORE, A., and A. LARSEN. 1964. Relative frequencies of ion clusters containing various numbers of ion pairs. *Radiat. Res.* 21:331.
- PARIKH, M. 1974. Possible investigation of molecular degradation using tunneling spectroscopy. Proceedings of the 32nd Annual Meeting of the Electron Microscope Society of America. Clailor's Publishing Div. 382.

- REIMER, L. 1965. Irradiation changes in organic and inorganic objects. *Lab. Invest.* **14**:1082.
- SCHRAM, B. L., F. J. DE HEER, M. J. VAN DER WIEL, and J. KISTENMAKER. 1965. Ionization cross sections for electrons (0.6–20 keV) in noble and diatomic gases. *Physica (Utrecht)*. **31**:94.
- SCHRAM, B. L., M. J. VAN DER WIEL, F. J. DE HEER, and H. R. MOUSTAFA. 1966. Absolute gross ionization cross sections for electrons (0.6–12 keV) in hydrocarbons. *J. Chem. Phys.* **44**:49.
- SIEGEL, G. 1972. Der Einfluss tiefer Temperaturen auf die Strahlenschädigung von organischen Kristallen durch 100 keV-Elektronen. *Z. Naturforsch.* **27a**:325.
- SPEHR, R., and H. SCHNABL. 1973. Zur Deutung der unterschiedlichen Strahlen-Empfindlichkeit organischer Moleküle. *Z. Naturforsch.* **28a**:1729.
- STENN, K., and G. F. BAHR. 1970. Specimen damage caused by the beam of the transmission electron microscope, a correlative reconsideration. *J. Ultrastruc. Res.* **31**:526.
- ZBINDEN, R. 1964. *Infrared Spectroscopy of High Polymers*. Academic Press, New York.